The Development of <100> Texture in Fe-Cr-Co-Mo Permanent Magnet Alloys

doi: 10.1109/20.79083

The Development of ⟨100⟩ Texture in Fe–Cr–Co–Mo Permanent Magnet Alloys

Satoshi Sugimoto, Hirohiko Satoh, Masuo Okada, and Motofumi Homma

Abstract—**The cold-rolled and recrystallization textures of Fe–Cr–Co–Mo permanent magnet alloys are described. The studied composition is Fe–30%Cr–15%Co–3%Mo (in wt%). The cold-rolled texture can be considered as {111}⟨110⟩, {111}⟨112⟩, {100}⟨110⟩, and {211}⟨110⟩, while the recrystallization texture can be considered as {111}⟨110⟩, {110}⟨112⟩, {211}⟨110⟩, and {110}⟨110⟩. The secondary recrystallization is caused by heat-treating the alloys in the sequence of α, α + γ, α + γ + σ, α phase region (HTSR). This results in a favorable texture of {110}⟨110⟩ and ⟨100⟩ direction, aligning along the transverse direction (TD) of the strips. The best magnetic properties obtained in this study are *Br* = 1.2 T (12.0 kG), *iHc* = 82.0 kAm^{-1} (1025 Oe), and (*BH*)max = 60.8 kJm^{-3} (7.6 MGOe) with TD alloys.**

Introduction

Fe–Cr–Co permanent magnets exhibit excellent magnetic properties comparable to those of the Alnico family, with good ductility [1]–[3]. The magnetic hardening of the alloys is induced by heat-treating within the miscibility gap, which produces a modulated structure consisting of two phases, an Fe–Co rich phase (α_1) and a Cr rich phase (α_2) [4]. A uniaxial magnetic anisotropy is usually induced by magnetic aging, which elongates the α_1 phase parallel to the applied field direction. In order to expand their applications, the enhancement of coercivity of the alloys is strongly demanded.

It is noted that the addition of Mo to these alloys increases the coercive force because of the anisotropic decomposition along the ⟨100⟩ directions [1], [5]. Good magnetic properties can be expected by utilizing the anisotropic decomposition to elongate more efficiently and aligning the α_1 phase along the applied field direction in ⟨100⟩ textured samples. This was done with an Fe–24%Cr–15%Co–3%Mo (in wt%) alloy in developing the ⟨100⟩ columnar structure [6] or with a ridge single-crystal Fe–22%Cr–18.5%Co–3%Mo alloy [7]. But it is very expensive to produce a columnar or single crystal.

Manuscript received July 17, 1990; revised January 2, 1991.

S. Sugimoto, M. Okada, and M. Homma are with the Department of Materials Science, Faculty of Engineering, Tohoku University, Sendai 980, Japan.

H. Satoh was with the Department of Materials Science, Faculty of Engineering, Tohoku University, Sendai 980, Japan. He is currently with the Electrical Sheet Division, Electrical Sheet Mill, Yawata Works, Nippon Steel Corporation, Kitakyushu 805, Japan.

IEEE Log Number 9143163.

It is known that the (110)[001] or (001)[100] texture in silicon steel is well developed by using a mixture of cold-rolling and annealing [8]. Since Fe–Cr–Co–Mo alloys have good ductilities, it can be expected to form a favorable texture by the same method. But few reports have been published concerning the cold-rolled and recrystallization texture of Fe–Cr–Co–Mo alloys. The purposes of this work are 1) to investigate the cold-rolled and recrystallization textures of Fe–Cr–Co–Mo alloys and 2) to obtain the favorable texture including the ⟨100⟩ direction and to obtain good magnetic properties also.

Experimental Procedures

The experimental procedure for the preparation of the alloys is shown in Fig. 1. The Fe–30%Cr–15%Co-3%Mo (in wt%) alloys were chosen for this investigation. The alloys were induction-melted in Ar atmosphere and cast into cylindrical specimens in a mold with an inside diameter of 25 mm. Chemical composition analysis of these alloys was made using the chemical wet method, and the results are shown in Fig. 1. The ingots were hot-forged to a bar of approximately 18 × 18 mm^2 in cross section. The bars were solution-treated at 1300°C for 30 min and then underwent hot-rolling eight or nine times at 1200°C at a thickness of 2 mm. The strips were reheated to 1200°C after each hot-rolling in order to prevent precipitation of the brittle σ phase.

The hot-rolled strips were cold-worked to strips in 1) one-step or 2) two-step methods after the heat treatment at 1250°C for 10 min. When the two-step cold-rolling method was adopted, the strips were annealed at 1100°C for 10 min after the first cold-rolling. The specimens were cut along the rolling direction (RD) and transverse direction (TD), respectively, from the final cold-rolled strips. After the final cold-rolling, the alloys were annealed for primary recrystallization at 1200°C or 1000°C for 10 min. These temperatures correspond to the a phase region of the alloy composition used. Some specimens were annealed for secondary recrystallization after primary recrystallization.

The alloys were heat treated for magnetic hardening after the annealing for recrystallization. The heat treatment for magnetic hardening is as follows: after the solution treatment at 1200°C for 1 h, the alloys were aged at 635°C for 20 min (TMT-1) and then at 615°C for 4 h

0018-9464/91/0500-3412$01.00 © 1991 IEEE

Fe-30Cr-15Co-3Mo

Fe	Cr	Co	Mo	Mn	S	O	N	C
bal.	29.7	15.0	3.05	0.053	0.066	0.0747	0.0119	0.0145

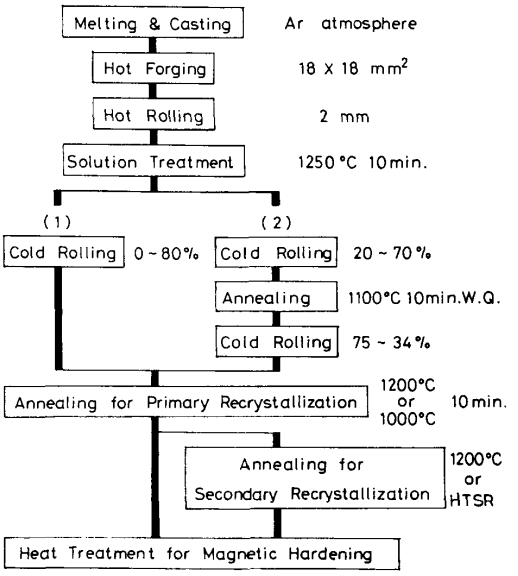

Fig. 1. Experimental procedure.

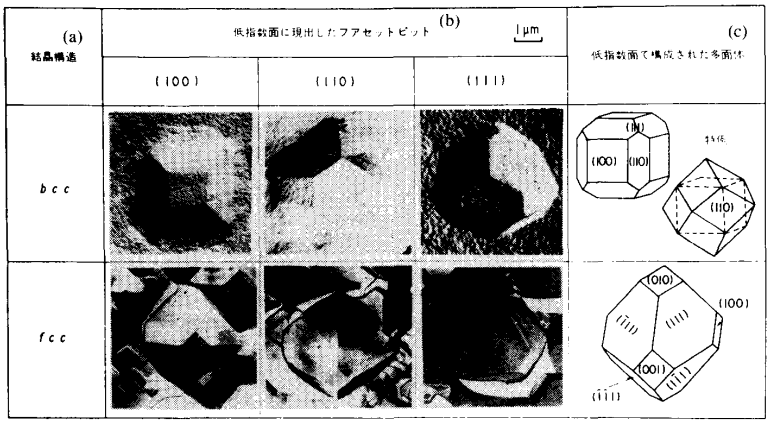

Fig. 2. Typical etching pits reported by Hayakawa *et al.* [11]. (a) Crystal structure. (b) Micro-facet pits with low indices. (c) Polyhedrons composed of low indices crystallographic plane.

(TMT-2) in a magnetic field of 160 kAm^{-1} (2 kOe). The alloys were then held at 610°C for 2 h, followed by controlled cooling at a rate of 4°C/h and held at 500°C for 10 h. The details are described in another work [9].

The magnetic properties were measured with an automatic fluxmeter. Texture was at first judged by the relative intensity (I/Io) of each X-ray peak diffracted by the surface of the cold-rolled and annealed strips, where Io exhibits the X-ray intensity of each diffracted peak from equiaxed alloys. If the I/Io value of a certain peak is over one, it means that the crystallographic plane corresponded the peak is one of the main crystallographic components for the strips. But when the grain size of the strips is large, this method cannot determine the texture. In order to determine the orientation of the grains, the shape of etching pits formed on the surface of the strips was observed. These etching pits consist of some crystallographic facets with low indices [10]. By measuring the normals to the facet of etching pits, the crystallographic orientation of the small region where the etching pits were embedded could be determined within the accuracy of 1° [10]. Typical etching pits reported by Hayakawa *et al.* [11] are shown in Fig. 2. In this study electrolytic and chemical etchings were used in order to produce distributed micro-

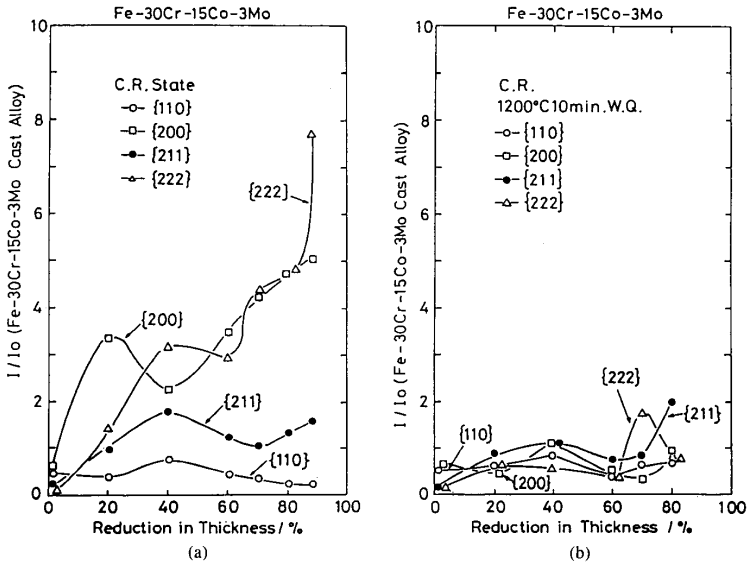

Fig. 3. Variation of relative X-ray diffracted intensity taken from (a) one-step cold-rolled and (b) annealed strips versus cold-rolling reduction in thickness.

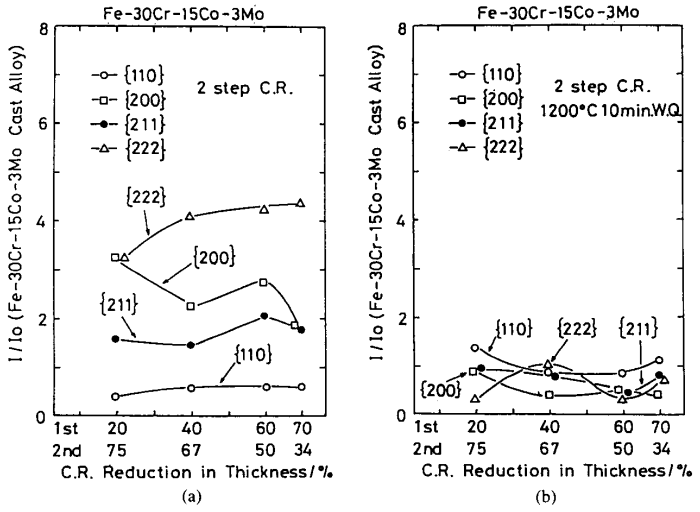

Fig. 4. Variation of relative X-ray diffracted intensity taken from (a) two-step cold-rolled and (b) annealed strips versus cold-rolling reduction in thickness.

pits uniformly. The reagent for these etchings are oxalic acid and aqua regia, respectively.

Results and Discussion

Cold-rolled and Recrystallization Texture

Fig. 3 shows the variation of relative X-ray diffracted intensity taken from a) one-step cold-rolled and b) annealed strips versus cold-rolling reduction in thickness. The intensity of {200} and {222} diffractions increases with the increasing rate of cold-rolling reduction and that of {211} diffraction is over one for all of cold-rolling reduction in thickness. It can be considered that {211}, {100}, and {111} planes are dominant on the surface of cold-rolling strips and that the volume of grains, which have {100} and {111} components, increase in the rolling plane with increasing cold-rolling reduction in thickness. But after the annealing for recrystallization, all diffractions are not so strong as those observed after cold-rolling. It can be said that strong texture is not developed after annealing.

Fig. 4 shows the variation of relative X-ray diffracted

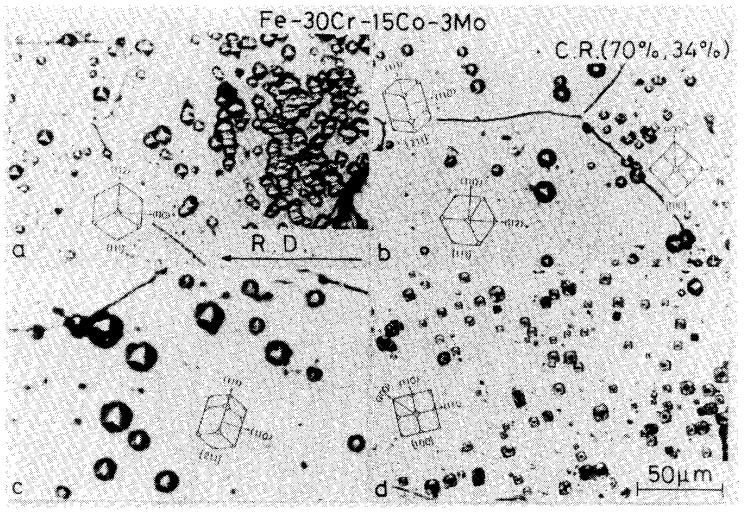

Fig. 5. Optical micrographs with etching pits taken from the rolling plane of (70%, 34%) two-step cold-rolled alloys.

intensity taken from a) two-step cold-rolled and b) annealed stips versus cold-rolled reduction in thickness. The variations of relative X-ray diffracted intensity versus reduction in thickness tend to follow the same manner as that for one-step cold-rolling shown in Fig. 3. Comparing Fig. 4(a) with Fig. 3(a), the relative X-ray diffracted intensity taken from two-step cold-rolled strips is not as strong as those taken from one-step cold-rolled strips because of the annealing after the first cold-rolling. But the intensity of {222}, {200}, and {211} diffractions are strong for all of the strips, which are two-step cold-rolled with various combinations of first and second cold-rolling. It can be said that the volume of the grains with {111}, {100}, and {211} components is large in the rolling plane after cold-rolling. But it is found that the annealed strips do not have the strong texture as shown in Fig. 4(b).

Fig. 5 shows the optical micrographs with the etching pits taken from the rolling plane of the two-step (70%, 34%) cold-rolled alloy, where 70%, 34% exhibits the combination of the first and the second rolling reduction in thickness. The shape of the etching pits indicates that the cold-rolled texture can be considered as {111}⟨110⟩, {111}⟨112⟩, {100}⟨110⟩, and {211}⟨110⟩. These textures are classified into two types reported in pure iron by C. S. Barrett [12]. The first type is the crystallographic texture that occurs by rotating {100}⟨110⟩ along ⟨110⟩, which is aligned parallel to the rolling direction. The second one is the texture that occurs by rotating {111}⟨110⟩ along ⟨111⟩, which exists normal to the rolling plane. It can be considered that the cold-rolled texture of Fe–Cr–Co–Mo alloys is the same as that reported in other BCC metals.

From Fig. 3(b) and Fig. 4(b), the I/Io values of various planes of annealed sheets are nearly one. It can be considered that the recrystallization texture is not so strong in annealed sheets and cannot be determined by X-ray diffraction. The shape of etching pits were then observed. Fig. 6 shows the optical micrographs with etching pits taken from the rolling plane of annealed sheets after two-step (70%, 34%) cold-rolling. The recrystallization texture can be considered as {110}⟨110⟩, {111}⟨110⟩, {111}⟨112⟩, and {100}⟨110⟩ from the shape of etching pits, which are similar to those of other reported BCC metals. For example, this crystallographic texture resembles the recrystallization texture of polycrystalline pure iron as reported by Kurjumov and Sachs [13].

The variation of the magnetic properties of the alloys versus two-step cold-rolling reduction is shown in Fig. 7, where RD and TD exhibit the magnetic properties measured along rolling direction and transverse direction, respectively. The difference of magnetic properties between RD and TD is small for all combinations of cold-rolling reduction, and the magnetic properties do not change drastically by changing the combination of rolling reduction. This observation means that the strong recrystallization texture cannot be developed. It can be said that the ⟨100⟩ direction does not align along one direction when using a combination of cold-rolling and annealing in the α phase region.

⟨100⟩ *Recrystallization Texture*

The grain that has {110}⟨110⟩ or {100}⟨110⟩ exists in the rolling plane after recrystallization. If the grain grows at the expense of the other grains by secondary recrystallization, the ⟨100⟩ directions align along TD or RD + 45°, respectively. In order to grow grains that have the favorable directions described previously, the heat treatment time was prolonged from 1 h to 40 h. But the resulted average gain size after heat treatment at 1200°C

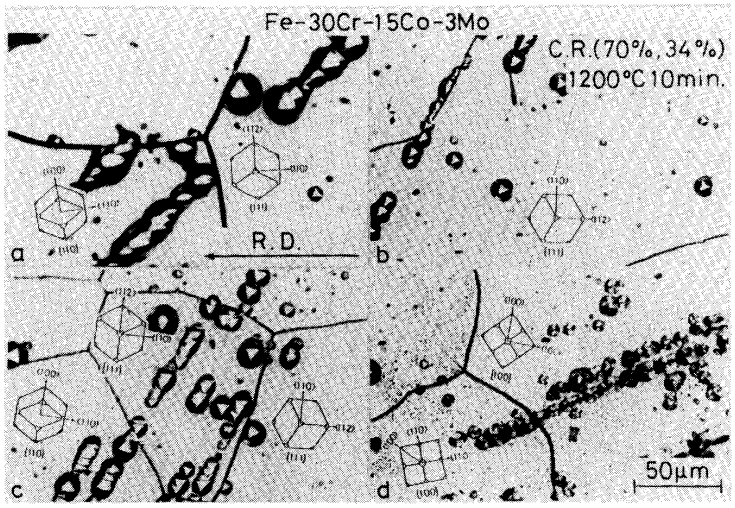

Fig. 6. Optical micrographs with etching pits taken from the rolling plane of annealed sheets after two-step (70%, 34%) cold-rolling.

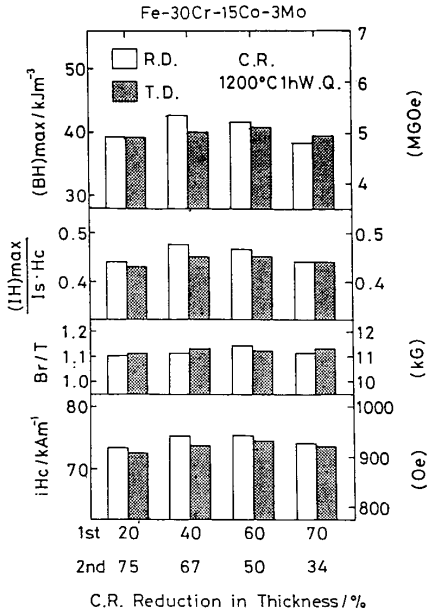

Fig. 7. Variation of magnetic properties of alloys versus four different combinations of two-step cold-rolling reduction in thickness.

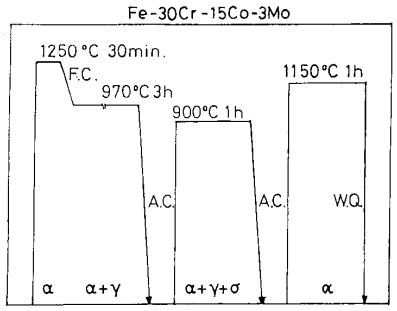

Fig. 8. Schematic diagram of the heat treatment for secondary recrystallization (HTSR).

for 40 h is 180 μm. The size of the grain is not very different from 140 μm, which is the average grain size after heat treatment for 1 h. It can be said that secondary recrystallization does not occur and ⟨100⟩ directions do not align along one direction in this method.

It is reported that the phase transformation among three different phase regions $\alpha + \gamma + \sigma$, $\alpha + \gamma$, and α is utilized for secondary recrystallization in preparation of Fe–Cr–Co single crystals [7]. In order to cause secondary recrystallization and give favorable texture, heat-treating the alloys in the sequence of α, $\alpha + \gamma$, $\alpha + \gamma + \sigma$, α, which is shown in Fig. 8, was adopted in this investigation. The heat treatment is as follows: after the annealing for the primary recrystallization at 1000°C for 10 min, the alloys are heat-treated first at 1250°C for 30 min, which is in an α phase region, followed by furnace cooling to 970°C and held there for 3 h, which is in $\alpha + \gamma$ phase region. The alloys were then heat-treated at 900°C for 1 h, which is in $\alpha + \gamma + \sigma$ region, and finally heat-treated at 1150°C for 1 h in an α phase region. Hereafter, this heat treatment for secondary recrystallization is abbreviated as HTSR.

Fig. 9 shows the magnetic properties of Fe–30Cr–15Co–3Mo alloys obtained by annealing only in an α phase region and by HTSR. The magnetic properties obtained by HTSR with TD alloys are iHc = 82 kAm^{-1} (1025 Oe) and (BH)max = 56.8 kJm^{-3} (7.1 MGOe). They are higher than those of RD alloys and alloys annealed only in an α phase region.

Fig. 10 shows the optical microstructures and the etching pits taken from the alloys after the annealing only in

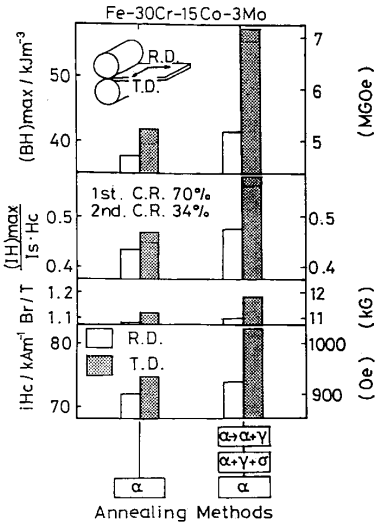

Fig. 9. Magnetic properties of Fe-30Cr-15Co-3Mo alloys obtained by annealing only in α phase region and by HTSR.

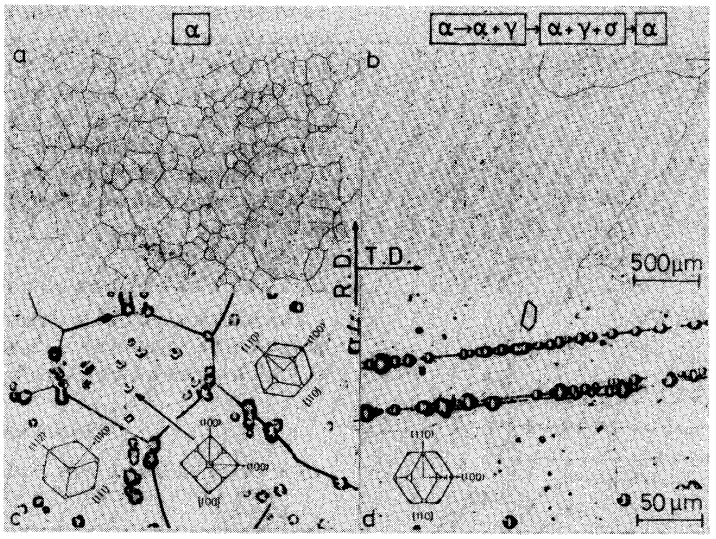

Fig. 10. Optical microstructures and etching pits taken from the alloys after the annealing only in α phase region [(a) and (c)] and HTSR [(b)] and (d)].

the α phase region ((a) and (c)) and HTSR ((b) and (d)). Although the average grain size of the alloy annealed only in the α phase region is 120 μm, the one by the HTSR is 2.6 mm. The grains obtained by HTSR are larger than those by the annealing in the α phase region. It can be considered that secondary recrystallization occurs efficiently in the alloys by the HTSR. From the shape of etching pits shown in Fig. 10(c), the grains of the alloys annealed in the α phase region have the {111} and {100} components. As a result the ⟨100⟩ directions exist randomly and do not align along one direction in the alloys. But the grains grown by HTSR have the {110} components with ⟨110⟩ directions along RD shown in Fig. 10(d). It can be considered that the texture composed mainly of {110}⟨110⟩ is obtained by the HTSR. In this texture, the ⟨100⟩ directions exist along TD, and good magnetic properties can be obtained with TD alloys.

Fig. 11 shows the magnetic properties of the alloys annealed by the HTSR after one-step cold-rolling. Good magnetic properties can be obtained with TD alloys after nearly 70% of cold-rolling reduction in thickness. Fig. 12 shows the magnetic properties of the alloys annealed by

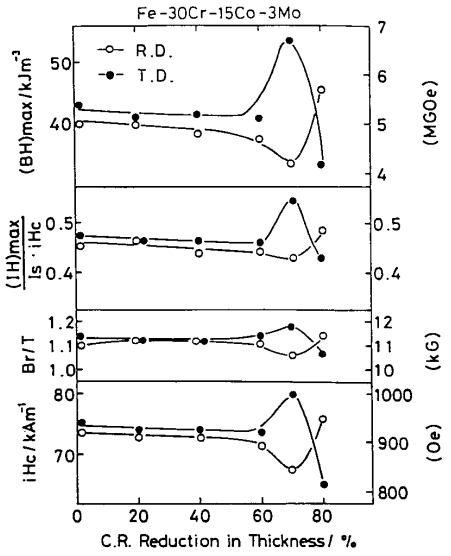

Fig. 11. Magnetic properties of alloys annealed by HTSR after one-step cold-rolling versus cold-rolling reduction in thickness.

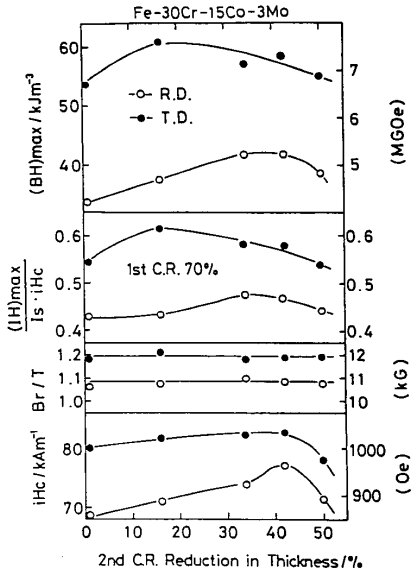

Fig. 12. Magnetic properties of alloys annealed by HTSR after two-step cold-rolling, whose first cold-rolling reduction is 70%, versus secondary reduction in thickness.

HTSR after two-step cold-rolling, whose first cold-rolling reduction rate is 70% versus secondary cold-rolling reduction in thickness. The energy products above 53.6 kJm^{-3} (6.3 MGOe) are obtained for almost all of the reduction rates of secondary cold-rolling reduction. The best magnetic properties, iHc = 82 kAm^{-1} (1025 Oe), (BH)max = 60.8 Jm^{-3} (7.6 MGOe), can be obtained by 70%, 15%) two-step cold-rolling with TD alloys.

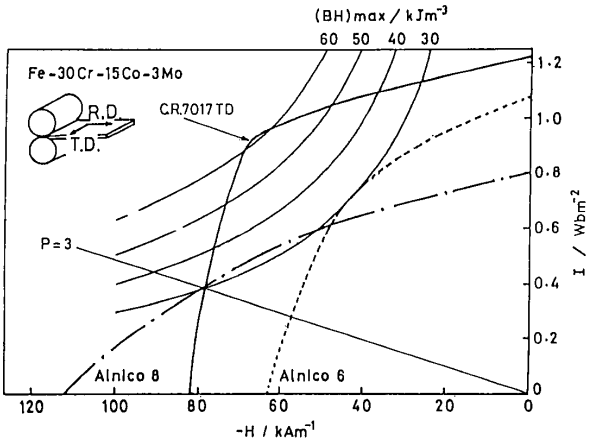

Fig. 13. Demagnetization curves of Fe-30Cr-15C0-3Mo alloy measured along RD and TD with those of Alnico 6 and 8.

The demagnetization curves of RD and TD alloys annealed by HTSR after two-step (70%, 17%) cold-rolling are shown in Fig. 13 in comparison with those of Alnico 6 and Alnico 8. TD alloys have good magnetic properties higher than those of RD alloy and Alnico 6. Although the coercivity of TD alloys is lower than that of Alnico 8, the higher magnetic flux can be obtained above $p = 3$ (where p is the permeance) with the advantage of cold formability. It can be concluded that this presently developed method is useful for the mass production of ⟨100⟩ aligned Fe–Cr–Co–Mo with high energy products comparable to Alnico 8.

Acknowledgment

The authors wold like to thank Dr. N. Ikuta for his suggestions. They also wish to thank Messrs. T. Shima and S. Torii for their assistance with any measurements.

Reference

[1] H. Kaneko, M. Homma, and K. Nakamura, "New ductile permanent magnet of Fe-Cr-Co system," in *AIP Conf. Proc.*, vol. 5, 1971, pp. 1088-92.
[2] S. Jin and G. Y. Chin, "Fe-Cr-Co magnets," *IEEE Trans. Magn.*, vol. MAG-23, pp. 3187-3192, 1987.
[3] M. Homma, M. Okada, T. Minowa, and E. Horikoshi, "Fe-Cr-Co permanent magnet alloys heat-treated in the ridge region of miscibility gap," *IEEE Trans. Magn.*, vol. MAG-17, pp. 3473-3478, 1981.
[4] M. Okada, G. Thomas, M. Homma, and H. Kaneko, "Microstructure and magnetic properties of Fe-Cr-Co alloys," *IEEE Trans. Magn.*, vol. MAG-14, pp. 245-252, 1978.
[5] R. Cremer and I. Pfeiffer, "Permanent magnet properties of Cr-Co-Fe alloys," *Physica*, vol. 80B, pp. 164-176, 1975.
[6] M. Homma, M. Okada, T. Minowa, and E. Horikoshi, "High-energy Fe-Cr-Co permanent magnets with (BH)max = 8-10 MGOe," *Appl. Phys. Lett.*, vol. 37, pp. 92-93, 1980.
[7] N. Ikuta, M. Okada, M. Homma, and T. Minowa, "Single crystal magnets," *J. Appl. Phys.*, vol. 54, pp. 5400-5403, 1983.
[8] N. P. Goss, U. S. Patent 1965559.
[9] S. Sugimoto, J. Honda, Y. Ohtani, M. Okada, and M. Homma, "Improvement of the magnetic properties of equiaxed Fe-Cr-Co-Mo hard magnets by two-step thermomagnetic treatment," *IEEE Trans. Magn.*, vol. MAG-23, pp. 3193-3195, 1987.
[10] T. Taoka, K. Ogasa, E. Furubayashi, and S. Takeuchi, "Some crys-

tallographic applications of goniomicroscope," (in Japanese), *J. Japan Inst. Metals*, vol. 30, pp. 820–826, 1966.
[11] H. Hayakawa and J. Imamura, "Microfacetpits method for determination of the crystallographic orientation in ferrite and austenite steel," *Bulletin Japan Inst. Metals*, vol. 18, pp. 282, (in Japanese), 1979.
[12] C. S. Barrett, *Structure of Metals*. New York: McGraw-Hill, 1952, pp. 463–473, pp. 500–502.
[13] G. Kurjumov, and W. G. Sachs, "Walz- und Rekristallisationstextur von Eisenblech," *Z. Physik*, vol. 62, pp. 592–599, 1930.

Satoshi Sugimoto was born in Shizuoka-Ken, Japan, on December 9, 1958. He received the B.E., M.E. and D.E. degrees in metallurgy from Tohoku University, Sendai, Japan, in 1982, 1984, and 1990, respectively.

He is currently a Research Associate with the Development of Materials Science at Tohoku University.

Dr. Sugimoto is a member of the Japan Institute of Metals and the Magnetic Society of Japan.

Hirohiko Satoh was born in Miyagi-Ken, Japan, on April 21, 1964. He received the B.E. and M.E. degrees in metallurgy from Tohoku University, Sendai, Japan, in 1988 and 1990, respectively.

He is currently a Researcher with the Electrical Sheet Division, Electrical Sheet Mill, Yawata Works, Nippon Steel Corporation.

Mr. Satoh is a member of the Japan Institute of Metals.

Masuo Okada was born in Tochigi-Ken, Japan, on July 5, 1948. He received the B.E. degree from Tohoku University, Japan, in 1971 and the Ph.D. degree in Metallurgy from the University of California, Berkeley, in 1978.

He is currently an Associate Professor with the Department of Materials Science at Tohoku University.

Dr. Okada is a member of the Japan Institute of Metals, the Magnetic Society of Japan, and the American Ceramic Society.

Motofumi Homma was born in Nagano-Ken, Japan, on June 13, 1936. He received the B.E. and Ph.D. degrees in metallurgy from Tohoku University, Sendai, Japan, in 1959 and 1966, respectively.

In 1964 he joined Tohoku University and is currently a Professor with the department of Materials Science, Faculty of Engineering.

Dr. Homma is a member of IEEE Magnetics Society, the Japan Institute of Metals, the Magnetic Society of Japan, and the Iron and Steel Institute of Japan.